Output field-quadrature measurements and squeezing in ultrastrong cavity-QED

New Journal of Physics
The open access journal at the forefront of physics

Deutsche Physikalische Gesellschaft DPG
IOP Institute of Physics

Published in partnership with: Deutsche Physikalische Gesellschaft and the Institute of Physics

CrossMark

OPEN ACCESS

RECEIVED
2 October 2016

ACCEPTED FOR PUBLICATION
10 November 2016

PUBLISHED
2 December 2016

PAPER

Output field-quadrature measurements and squeezing in ultrastrong cavity-QED

Roberto Stassi[1,2,6], **Salvatore Savasta**[2,3], **Luigi Garziano**[2,3], **Bernardo Spagnolo**[1,4] **and Franco Nori**[2,5]

[1] Dipartimento di Fisica e Chimica, Group of Interdisciplinary Theoretical Physics, Università di Palermo and CNISM, Viale delle Scienze, Edificio 18, I-90128 Palermo, Italy
[2] CEMS, RIKEN, Saitama 351-0198, Japan
[3] Dipartimento di Fisica e di Scienze della Terra, Università di Messina, Viale F. Stagno d'Alcontres 31, I-98166 Messina, Italy
[4] Istituto Nazionale di Fisica Nucleare, Sezione di Catania, Italy
[5] Physics Department, The University of Michigan, Ann Arbor, MI 48109-1040, USA
[6] Author to whom any correspondence should be addressed.

E-mail: rstassi@unime.it

Keywords: quadrature measurements, squeezing, ultrastrong cavity-QED

Abstract

We study the squeezing of output quadratures of an electro-magnetic field escaping from a resonator coupled to a general quantum system with arbitrary interaction strengths. The generalized theoretical analysis of output squeezing proposed here is valid for all the interaction regimes of cavity-quantum electrodynamics: from the weak to the strong, ultrastrong, and deep coupling regimes. For coupling rates comparable or larger then the cavity resonance frequency, the standard input–output theory for optical cavities fails to calculate the variance of output field-quadratures and predicts a non-negligible amount of output squeezing, even if the system is in its ground state. Here we show that, for arbitrary interaction strength and for general cavity-embedded quantum systems, no squeezing can be found in the output-field quadratures if the system is in its ground state. We also apply the proposed theoretical approach to study the output squeezing produced by: (i) an artificial two-level atom embedded in a coherently-excited cavity; and (ii) a cascade-type three-level system interacting with a cavity field mode. In the latter case the output squeezing arises from the virtual photons of the atom-cavity dressed states. This work extends the possibility of predicting and analyzing the results of continuous-variable optical quantum-state tomography when optical resonators interact very strongly with other quantum systems.

1. Introduction

Recently, a new regime of cavity quantum electrodynamics (QED) has been experimentally reached in different solid state systems and spectral ranges [1–8]. In this so-called ultrastrong coupling (USC) regime, where the light–matter coupling rate becomes an appreciable fraction of the unperturbed resonance frequency of the system, the routinely invoked rotating wave approximation (RWA) is no longer applicable and the antiresonant terms significantly change the standard cavity-QED scenarios [9–18].

It has been shown that, in this USC regime, the correct description of the output photon flux, as well as of higher-order Glauber's normal-order correlation functions, requires a proper generalization of the input–output theory for resonators [13, 19, 20]. Application of the standard input–output picture to the USC regime would predict an unphysical continuous stream of output photons for a system in its ground state $|G\rangle$. This result stems from the finite number of photons which are present in the ground state due to the counter-rotating terms in the interaction Hamiltonian [21]. Specifically, it has been shown [13, 22] that the photon rate emitted by a resonator and detectable by a photo-absorber is no longer proportional to $\langle \hat{a}^{\dagger}(t)\hat{a}(t)\rangle$ (as predicted by the standard input–output theory), where $\hat{a}$ and $\hat{a}^{\dagger}$ are the photon destruction and creation operators of the cavity mode, but to $\langle \hat{x}^{-}(t)\hat{x}^{+}(t)\rangle$, where $\hat{x}^{+}(t)$ is the positive frequency component of the quadrature operator

$\hat{x}(t) = \hat{a}(t) + \hat{a}^{\dagger}(t)$ and $\hat{x}^{-}(t) = (\hat{x}^{+}(t))^{\dagger}$, which can be different from the bare photon creation an destruction operators. When the coupling rate is not a negligible fraction of the bare resonance frequencies, the correct separation into positive and negative frequency operators can be performed only by including the influence of the interaction Hamiltonian. This separation can be easily performed after the diagonalization of the total system Hamiltonian.

Direct photon counting experiments provide information about the mean photon number and higher-order normal-order correlations. However a complete quantum tomography of the electro-magnetic field (see, e.g., [23]) requires phase-sensitive measurements which are based on homodyne or heterodyne detection [24, 25]. These techniques enable the measurements of the mean field quadratures and their variance, e.g., $\langle \hat{x} \rangle$ and $\langle \hat{x}^2 \rangle - \langle \hat{x} \rangle^2$. More generally, for an electro-magnetic field-mode, it is possible to define two complementary field-quadratures $\hat{Q}_1$ and $\hat{Q}_2$ with $[\hat{Q}_1, \hat{Q}_2] = 1$, as $\hat{Q}_1 = \hat{a}e^{-i\phi} + \hat{a}^{\dagger}e^{i\phi}$ and $\hat{Q}_2 = -i(\hat{a}e^{-i\phi} - \hat{a}^{\dagger}e^{i\phi})$. In a coherent state of an electro-magnetic field mode, the quantum fluctuations of the two field-quadratures $\hat{Q}_1$ and $\hat{Q}_2$ are equal ($\Delta\hat{Q}_1 = \Delta\hat{Q}_2 = 1$, where $\Delta\hat{Q}_i = \langle \hat{Q}_i^2 \rangle - \langle \hat{Q}_i \rangle^2$) and minimize the uncertainty product given by Heisenberg's uncertainty relation $\Delta\hat{Q}_1\, \Delta\hat{Q}_2 = 1$ (we use $\hbar = 1$). These zero-point fluctuations represent the standard quantum limit to the reduction of noise in a signal. Other minimum-uncertainty states are possible, and these occur when fluctuations in one quadrature are squeezed at the expense of increased fluctuations in the other one [26]. Light squeezing can be realized in various nonlinear optical processes, such as parametric down-conversion, parametric amplification, and degenerate four-wave mixing [27–31] or in presence of time-dependent boundary conditions [32–35]. Squeezed states of light belong to the class of nonclassical states of light. Having a less noisy quadrature, squeezed light has applications in optical communication [36] and measurements [36–40] and is a primary resource in continuous variable quantum information processing [38]. Squeezing of the electromagnetic field has been achieved in a variety of systems operating in the optical and microwave regimes. A noise reduction of −10 dB (−13 dB is the estimation of squeezing after correction for detector inefficiency) has been achieved in the experiment [41]. More recently, a few experiments with superconducting circuits [34, 42] have demonstrated the possibility of obtaining much stronger squeezing in microwave fields [43].

Here we present a theory of quadrature measurements of the output field escaping from a resonator coupled to a generic matter system with arbitrary interaction strength, and we apply it to the analysis of squeezing. In cavity-QED systems, the squeezing effect has been usually studied by using the rotating-wave approximation [44–49]. While in the USC regime the positive frequency component $\hat{x}^{+}$ is different from $\hat{a}$ (it may contain contributions from the creation operator of the cavity field), the quadrature operator $\hat{x} = \hat{a} + \hat{a}^{\dagger} = \hat{x}^{+} + \hat{x}^{-}$ is independent of the light–matter interaction strength. Hence, at a first sight, one may expect that, in contrast to Glauber's correlation functions, quadrature measurements can be analyzed by applying the standard input–output theory [50, 51]. Here we show that this is not the case: application of the standard input–output picture to the analysis of quadrature measurements in the USC regime leads to incorrect results. We also observe that the calculation of quadrature expectation values by means of the generalized input–output relations (working for arbitrary light–matter coupling) presents some additional complications compared to that of normal-order correlations. In particular, the resulting quadrature expectation values contain products of system and input operators and thus cannot be directly derived within the master equation approach. The present analysis is of particular interest for the description of measurements in circuit-QED systems, where output quadrature measurements are generally employed since efficient microwave photon-counting detectors are not currently available. However, well-developed linear amplifiers allow for the efficient measurement of the field-quadrature amplitudes [25, 42, 52, 53]. Using input–output theory [51], one can show that the full information about the intracavity field-mode is contained in the moments and cross-correlations of the time-dependent output quadrature amplitudes. It has been demonstrated experimentally that correlation-function measurements based on quadrature amplitude detection are a powerful tool to characterize quantum properties of propagating microwave-frequency radiation fields [52]. Hence a general method to calculate these time-dependent moments, when the resonator interacts with one or more artificial atoms in the USC regime, is highly desirable for the analysis of the output microwave field in circuit-QED systems.

We apply the theoretical framework developed here to analyze three different cases: (i) we analyze the output field-quadratures for a system in its ground state. It is know that the ground state of a system in the USC regime is a squeezed vacuum state [19], where the amount of squeezing depends on the coupling strength and on the detuning between the cavity mode and the matter-system resonances. A correlation-function analysis of the quadratures of microwave fields has been exploited for measurements of vacuum fluctuations and weak thermal fields [54]. Hence the question arises if it is possible to detect such vacuum squeezing. Here, under quite general hypotheses, we demonstrate that for arbitrary cavity-embedded quantum systems, independently on the coupling rate, no squeezing can be found in the output field quadratures if the system is in its ground state. (ii) We study a coherently excited cavity interacting with an artificial two-level atom. Recently, it has been shown

that superconducting artificial atoms, subject to parity-symmetry-breaking and ultrastrong coupled to superconducting resonators, can display two-photon vacuum Rabi oscillations [22]. However, two-photon correlations cannot directly be detected in these systems. We show that quadrature-noise measurements can provide an alternative direct probe. This process can give rise to a high degree of squeezing in presence of a single two-level system, just exciting the qubit with a classical microwave pulse. (iii) As a further example of the developed framework, we analyze the output squeezing from a resonator interacting with a cascade-type three-level system.

We start out, in section 2, with the squeezing of the ground state of the Rabi Hamiltonian. In section 3 we present a theoretical framework of the output field quadratures. In section 4 this theoretical approach is applied to single-atom USC cavity-QED systems. Finally, in section 5 we present our conclusions.

2. Squeezing of the ground state of the Rabi Hamiltonian

The Hamiltonian of the quantum Rabi model ($\hbar = 1$) [55, 56] is given by

$$\hat{H}_{\mathrm{R}} = \omega_{\mathrm{c}}\, \hat{a}^{\dagger}\hat{a} + \frac{\omega_{\mathrm{q}}}{2}\hat{\sigma}_z + \Omega_{\mathrm{R}}\,(\hat{a}^{\dagger} + \hat{a})\,\hat{\sigma}_x, \tag{1}$$

where $\hat{a}$ and $\hat{a}^{\dagger}$ are, respectively, the annihilation and creation operators for the cavity field of frequency ω_{c}. The Pauli matrices are defined as $\hat{\sigma}_z = |e\rangle\langle e| - |g\rangle\langle g|$ and $\hat{\sigma}_x = \hat{\sigma}_+ + \hat{\sigma}_- = |e\rangle\langle g| + |g\rangle\langle e|$, in terms of the atomic ground ($|g\rangle$) and excited ($|e\rangle$) states. The parameter ω_{q} describes the transition energy of the two-level system and Ω_{R} is the coupling energy between the atomic transition and the cavity field.

Owing to the presence of the so-called counter-rotating terms, $\hat{a}\hat{\sigma}_-$ and $\hat{a}^{\dagger}\hat{\sigma}_+$, in the Rabi Hamiltonian, the operator describing the total number of excitations, $\hat{N} = \hat{a}^{\dagger}\hat{a} + |e\rangle\langle e|$, does not commute with $\hat{H}_{\mathrm{R}}$ and as a consequence the eigenstates of $\hat{H}_{\mathrm{R}}$ do not have a definite number of excitations [21], however the system described by the Hamiltonian in equation (1) conserves the parity of the number of excitations. For instance the resulting ground state, in terms of the bare cavity and qubit states, is a superposition of an even number of excitations [21],

$$|G\rangle \equiv |\tilde{0}\rangle = \sum_{k=0}^{\infty}(c^{\tilde{0}}_{g,2k}|g,\, 2k\rangle + c^{\tilde{0}}_{e,k}|e,\, 2k+1\rangle), \tag{2}$$

where the second entry in the kets provides the photon number. The coefficients of this expansion can be calculated diagonalizing numerically the Rabi Hamiltonian in equation (1) (see, e.g., [21, 22]). When the coupling rate Ω_{R} is much smaller than the bare resonance frequencies of the two subsystems ω_{c} and ω_{q}, only $c^{\tilde{0}}_{g,0}$ is significantly different from zero and the ground state reduces to $|\tilde{0}\rangle \simeq |g,\, 0\rangle$, which is that of the Jaynes–Cummings model, derived from the Rabi Hamiltonian after dropping the counter-rotating terms. When the coupling rate Ω_{R} approaches and exceed 10% of the bare frequencies of the subsystems, that is USC regime, contributions with $k \neq 0$ in equation (2) become not negligible. One consequence is that the mean photon number in the ground state $\langle\tilde{0}|\hat{a}^{\dagger}\hat{a}|\tilde{0}\rangle$ becomes different from zero. Moreover, the ground state displays a certain amount of photon squeezing. Considering the intracavity-field quadrature $\hat{q}_2 = \mathrm{i}(\hat{a}^{\dagger} - \hat{a})$, its variance $s_2 = \langle\tilde{0}|\hat{q}_2^2|\tilde{0}\rangle - \langle\tilde{0}|\hat{q}_2|\tilde{0}\rangle^2$ (notice that $\langle\tilde{0}|\hat{q}_2|\tilde{0}\rangle = 0$) turns out to be below the standard quantum limit value 1.

Figure 1 displays the numerically calculated $s_2^{(n)} = s_2 - 1$ as a function of the normalized coupling $\Omega_{\mathrm{R}}/\omega_{\mathrm{c}}$ and detuning $\Delta/\omega_{\mathrm{c}} = (\omega_{\mathrm{q}} - \omega_{\mathrm{c}})/\omega_{\mathrm{c}}$. For small values of the normalized coupling, the variance approaches the standard quantum limit.

We notice that, increasing $\Omega_{\mathrm{R}}/\omega_{\mathrm{c}}$, the variance decreases below the standard quantum limit, reaching a lowest value of about -0.35, at $\Omega_{\mathrm{R}}/\omega_{\mathrm{c}} \simeq 1.05$ and at a positive detuning $\Delta/\omega_{\mathrm{c}} \simeq 0.76$. Further increasing the coupling, especially at zero and negative detuning, results into an increase of the variance s_2, caused by quite large contributions in $|\tilde{0}\rangle$ of terms with an odd number of photons.

This noise increase can be understood noticing that the noise reduction originates from the terms $\langle\psi|\hat{a}^2|\psi\rangle$, and the operator $\hat{a}^2$ connects only terms in the quantum states $|\psi\rangle$ differing by two photons. Hence squeezing can be larger for states with either an even or an odd number of photons. In the next section we will show that such a ground-state squeezing actually does not give rise to an observable output squeezing.

3. Output field quadratures

According to the input–output theory for general localized quantum systems interacting with a propagating quantum field, the output field operator can be related through a boundary condition to a system operator and the input field operators [57]. In order to be specific, we consider the case of a system coupled to a semi-infinite transmission line [57], although the results obtained can be applied or extended to a large class of systems. While the resonator can be ultrastrongly coupled to a localized quantum system, its interaction with the propagating

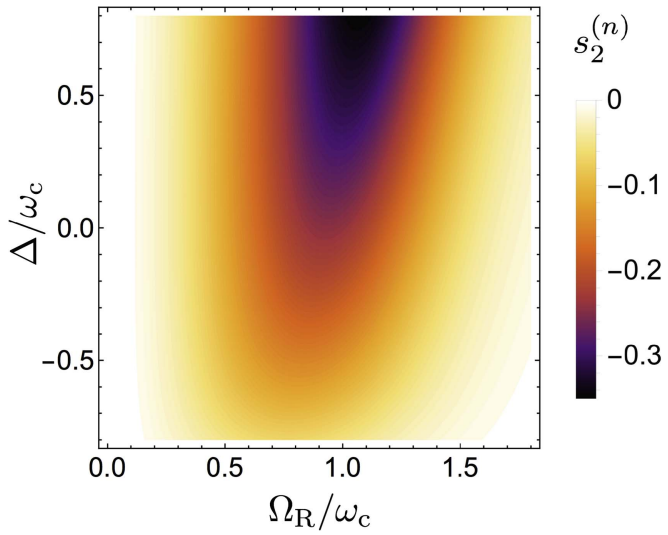

Figure 1. Normally-ordered variance $s_2^{(n)} = s_2 - 1$ of the cavity-field quadrature $\hat{x}_2 = \mathrm{i}(\hat{a}^\dagger - \hat{a})$, calculated in the ground state $|\tilde{0}\rangle$ of the Rabi Hamiltonian, as a function of the normalized coupling rate Ω_R/ω_c and cavity-atom detuning $\Delta/\omega_c = (\omega_q - \omega_c)/\omega_c$.

quantum field (e.g., the transmission line) is weak. To derive the *input–output* relations we couple the system to a quantum field made of an assembly of harmonic oscillators. The total Hamiltonian of the system can be written as

$$\hat{H} = \hat{H}_S + \hat{H}_F + \hat{H}_{SF}, \tag{3}$$

where $\hat{H}_S$ and $\hat{H}_F$ are the system and field Hamiltonian and where the interaction between the system and the field can be expressed in the rotating wave approximation as

$$\hat{H}_{SF} = \mathrm{i}\int_0^\infty \mathrm{d}\omega\, k(\omega)\sqrt{\frac{v\hbar\omega}{2}}\,[\hat{X}^-\hat{b}(\omega) - \hat{X}^+\hat{b}^\dagger(\omega)], \tag{4}$$

where v is the speed of the traveling field, e.g., the speed of light in the transmission line.

In the above equation, $\hat{b}(\omega)$ and $k(\omega)$ are the annihilation operator and the spectral density for the harmonic oscillators that describe the output field, $\hat{X}^+$ and $\hat{X}^-$ are the *positive* and *negative* frequency components of the generic system operator $\hat{X}$ coupled to the field. These components can be obtained expressing $\hat{X}$ in the eigenvectors basis of $\hat{H}_S$ as

$$\hat{X}^+ = \sum_{i<j} X_{ij}\ |i\rangle\langle j|, \tag{5}$$

and $\hat{X}^- = (\hat{X}^+)^\dagger$. Here the eigenstates of $\hat{H}_S$ are labeled according to their eigenvalues such that $\omega_k > \omega_j$ for $k > j$. We observe that the rotating wave approximation used in equation (A4) is based on the separation into positive and negative frequency operators of the system operator $\hat{X}$ after the system diagonalization. The standard RWA is instead based on the separation into bare positive (destruction) and negative (creation) components of the field operator coupled to the external modes, without including its interaction with other components of the system.

The *positive* frequency component of the input and output fields can be written as

$$\hat{A}^+_{\mathrm{in(out)}}(t) = \frac{1}{2}\int_0^\infty \mathrm{d}\omega\sqrt{\frac{\hbar}{\pi\omega}}\,\hat{b}(\omega, t')\exp[-\mathrm{i}\omega(t - t'], \tag{6}$$

while the *negative* frequency component $\hat{A}^-_{\mathrm{in(out)}} = (\hat{A}^+_{\mathrm{in(out)}})^\dagger$, so that $\hat{A}_{\mathrm{in(out)}}(t) = \hat{A}^+_{\mathrm{in(out)}}(t) + \hat{A}^-_{\mathrm{in(out)}}(t)$, in which $t' < t$ (the input) is a fixed initial time and $t' > t$ (the output) is assumed to be in the remote future [57]. Formally solving the Heisenberg equations of motion for $\hat{b}(\omega)$, the input–output relations for the positive and negative components of the fields can be obtained [22]

$$\hat{A}^\pm_{\mathrm{out}}(t) = \hat{A}^\pm_{\mathrm{in}}(t) - \sqrt{\gamma}\hat{X}^\pm(t), \tag{7}$$

where for the sake of simplicity the first Markov approximation, $k(\omega) = \sqrt{2\gamma/\pi}$, has been adopted. However, the present analysis can be easily extended beyond this approximation. Equation (7) shows that the positive frequency output operator can be expressed in terms of the positive frequency input operator and the positive frequency system operator coupled to the propagating field. If the system consists of an empty single-mode resonator, then $\hat{X}^+ \propto \hat{a}$, being $\hat{a}$ the destruction operator of the cavity mode. If instead the cavity mode is

coupled to another quantum system, e.g., an atom, $\hat{X}^+$ will be different from $\hat{a}$, and may also contain contributions from $\hat{a}^\dagger$. In this case, the positive component of the output field may contain contributions from the creation operator of the cavity field, in contrast to ordinary quantum optical input–output relationships [27, 51].

We define the output quadrature operators $\hat{Q}_1(t)$ and $\hat{Q}_2(t)$ as

$$\hat{Q}_1(t) = \hat{A}^+_{\rm out}(t)e^{-i\Gamma(t)} + \hat{A}^-_{\rm out}(t)e^{i\Gamma(t)}$$
$$\hat{Q}_2(t) = -\,i[\hat{A}^+_{\rm out}(t)e^{-i\Gamma(t)} - \hat{A}^-_{\rm out}(t)e^{i\Gamma(t)}] \tag{8}$$

so that

$$\hat{A}^\pm_{\rm out}(t) = \frac{1}{2}[\hat{Q}_1(t) \pm i\hat{Q}_2(t)]\exp[i\Gamma(t)], \tag{9}$$

where $\Gamma(t) = \Omega t + \varphi$. Here Ω and φ are, respectively, the frequency and the phase of the local oscillator field employed for the squeezing measurements [29]. It is possible to change from one quadrature to the other by applying a $\pi/2$ rotation to one of the two quadratures, e.g., by changing the reference phase φ.

Let us now consider the field-quadrature variance $S_i(t, \tau) = \langle \hat{Q}_i(t), \hat{Q}_i(t+\tau)\rangle$. Using equation (9), it can be expressed in terms of the output operators,

$$S_{\rm i}(t, \tau) = \langle \hat{A}^+_{\rm out}(t)\hat{A}^+_{\rm out}(t+\tau)\rangle e^{-2i\Gamma} + \langle \hat{A}^-_{\rm out}(t)\hat{A}^-_{\rm out}(t+\tau)\rangle e^{2i\Gamma}$$
$$+ \langle \hat{A}^+_{\rm out}(t)\hat{A}^-_{\rm out}(t+\tau)\rangle + \langle \hat{A}^-_{\rm out}(t)\hat{A}^+_{\rm out}(t+\tau)\rangle. \tag{10}$$

By using the input–output relation (7), each term in the above equation can be written in terms of input and system operators. For example, the first expectation value in the r.h.s. of equation (10) becomes,

$$\langle \hat{A}^+_{\rm out}(t)\hat{A}^+_{\rm out}(t+\tau)\rangle = \langle \hat{A}^+_{\rm in}(t)\hat{A}^+_{\rm in}(t+\tau)\rangle + \gamma\langle \hat{X}^+(t)\hat{X}^+(t+\tau)\rangle$$
$$- \sqrt{\gamma}\langle \hat{A}^+_{\rm in}(t)\hat{X}^+(t+\tau)\rangle - \sqrt{\gamma}\langle \hat{X}^+(t)\hat{A}^+_{\rm in}(t+\tau)\rangle. \tag{11}$$

We observe that equation (11) contains expectation values involving products of input and system operators. Even considering the important case of a vacuum input port, the mixed term $\langle \hat{A}^+_{\rm in}(t)\hat{X}^+(t+\tau)\rangle$ is in general different from zero and cannot be directly calculated by the master equation approach, which does not calculate mixed bath-system correlations. This problem can be solved by deriving the commutation relations between system and input operators. By using equation (6) and the expression of the field operator $\hat{b}(\omega)$, obtained from solving the Heisenberg equation, we arrive at the following commutation relation between any system variable $\hat{Y}(t)$ and the input fields $\hat{A}^\pm_{\rm in}(t)$

$$[\hat{Y}(t), \hat{A}^\pm_{\rm in}(s)] = \sqrt{\gamma}\, u(t-s)[\hat{Y}(t), \hat{X}^\pm(s)], \tag{12}$$

where $u(t-s)$ is equal to 1 if $t > s$, $\frac{1}{2}$ if $t = s$, and 0 if $t < s$. This commutation relation, which holds for arbitrary light–matter couplings, can be considered to be the generalization of an analogous commutation relation obtained within the standard input–output framework [50]. Its derivation is described in appendix A.

Making use of the *input–output* relations (7) and of the commutation relations (12), we can proceed to calculate the output field quadrature variances $S_i(t, \tau) = \langle \hat{Q}_i(t), \hat{Q}_i(t+\tau)\rangle$ in terms of correlation functions involving only input operators or system operators. Here we used $\langle \hat{A}, \hat{B}\rangle = \langle \hat{A}\hat{B}\rangle - \langle \hat{A}\rangle\langle \hat{B}\rangle$. Considering an input in a vacuum or a coherent state, the field-quadrature variances can be expressed as

$$S_1(t, \tau) = \gamma[\mathcal{T}\langle \hat{X}^+(t+\tau), \hat{X}^+(t)\rangle e^{-2i\Gamma(t)} + \mathcal{T}\langle \hat{X}^-(t), \hat{X}^-(t+\tau)\rangle e^{2i\Gamma(t)}$$
$$+ \langle \hat{X}^-(t+\tau), \hat{X}^+(t)\rangle + \langle \hat{X}^-(t), \hat{X}^+(t+\tau)\rangle]$$
$$+ \langle \hat{A}^+_{\rm in}(t), \hat{A}^-_{\rm in}(t+\tau)\rangle, \tag{13}$$

where $\mathcal{T}$ is the time-ordering operator that rearranges the creation operators in the forward time, and also the annihilation operators in the backward temporal order. To obtain S_2 we can apply a $\pi/2$ rotation to equation (13). For equal-time correlation functions ($\tau = 0$), we have

$$S_1(t) = \gamma[\langle \hat{X}^+(t), \hat{X}^+(t)\rangle e^{-2i\Gamma(t)} + \langle \hat{X}^-(t), \hat{X}^-(t)\rangle e^{2i\Gamma(t)} + 2\langle \hat{X}^-(t), \hat{X}^+(t)\rangle]$$
$$+ \langle \hat{A}^+_{\rm in}(t), \hat{A}^-_{\rm in}(t)\rangle. \tag{14}$$

The last term in equation (14) $\langle \hat{A}^+_{\rm in}, \hat{A}^-_{\rm in}\rangle$ describes the quantum noise of the input in the vacuum state. We observe that, according to equation (5), the operator $\hat{X}^+$ can induce only downward transitions from higher energy to lower energy levels. Hence, when it is applied to the ground state, it automatically gives zero:

$$\hat{X}^+|G\rangle = 0. \tag{15}$$

If the system starts in its ground state, in the presence of a vacuum input, it will remain there. Using then equation (15), the term $\langle \hat{X}^-(t), \hat{X}^+(t)\rangle$ in equation (14) becomes zero and the output noise in equation (14) coincides with the input one: $S_1(t) = \langle \hat{A}_{\rm in}^+(t)\hat{A}_{\rm in}^-(t)\rangle$. From equations (14) and (15) we can thus formulate the following general statement: *Any open system in its ground state, i.e.,* $\hat{X}^+ |0\rangle = 0$, *does not display any output squeezing, even if its ground state is a squeezed state*. Equation (14) holds for general open quantum systems, independently on their composition in subsystems and the degree of interaction among the different subsystems. This absence of output ground-state squeezing has been previously shown in different interacting harmonic systems [19, 58, 59].

In order to compare this result with previous descriptions for optical resonators, we consider the case where $\hat{X}$ describes the field of a single-mode cavity: $\hat{X} = X_0\hat{x} = X_0(\hat{a} + \hat{a}^\dagger)$. Here X_0 denotes the zero-point fluctuation amplitude of the resonator. Equation (14) can be expressed as

$$\begin{aligned} S_1(t) &= \gamma X_0^2[\langle \hat{x}^+(t), \hat{x}^+(t)\rangle e^{-2i\Gamma(t)} + \langle \hat{x}^-(t), \hat{x}^-(t)\rangle e^{2i\Gamma(t)} + 2\langle \hat{x}^-(t), \hat{x}^+(t)\rangle] \\ &\quad + \langle \hat{A}_{\rm in}^+(t), \hat{A}_{\rm in}^-(t)\rangle. \end{aligned} \tag{16}$$

If the interaction of the resonator with other quantum systems is not in the USC regime, $\hat{x}^+ = \hat{a}$ and $\hat{x}^- = \hat{a}^\dagger$. The noise reduction with respect to the vacuum input can be expressed in terms of the following normally-ordered variance

$$S_i^{(n)}(t) = \frac{S_i(t) - \langle \hat{A}_{\rm in}^+(t), \hat{A}_{\rm in}^-(t)\rangle}{\gamma X_0^2}. \tag{17}$$

For a resonator not in the USC regime, an ideally squeezed quadrature corresponds to $S_i^{(n)} = -1$, while for a resonator in the ground state $S_i^{(n)} = 0$.

4. Squeezing of output field-quadratures in the USC regime

Here we apply the theoretical framework developed in section 3 to study the output field-quadrature variances in single-atom USC cavity-QED systems. We first consider the case of a flux qubit artificial atom coupled to a $\lambda/2$ superconducting transmission-line resonator, when the frequency of the resonator is near one-half of the atomic transition frequency (see figure 2). Recently it has been shown [60] that this regime can strongly modify the concept of vacuum Rabi oscillations, enabling two-photon exchanges between the qubit and the resonator. Here we show that such configuration can provide a very large amount of squeezing, although the system has only one artificial atom and displays a moderate coupling rate $\Omega_{\rm R}/\omega_{\rm c} \sim 0.1$. Then, we will study the output squeezing of a cascade three-level system where only the upper transition is coupled to the optical resonator.

In order to describe a realistic system, the dissipation channels need to be taken into account. For this reason all the dynamical evolutions displayed below have been numerically calculated solving the master equation $\dot{\hat{\rho}}(t) = i[\hat{\rho}(t), H] + \sum_i \mathcal{L}_i\hat{\rho}(t)$ [22, 61, 62], where $\mathcal{L}_i$ is a Liouvillian superoperator describing the cavity and atomic system losses (see appendix A). All calculations have been carried out by considering zero temperature reservoirs.

4.1. Two-photon Rabi oscillations

We now consider a flux qubit ultrastrongly coupled to a coplanar resonator [2]. This quantum circuit is analogous to a cavity-QED system, where the flux qubit with its discrete anharmonic energy levels represents the artificial atom and the coplanar resonator the optical cavity (see figure 2). Recently it has been shown that this system paves the way to anomalous vacuum Rabi oscillations, where two or more photons are jointly and reversibly emitted and reabsorbed by the qubit [60, 63].

This quantum circuit can be described by the following extended Rabi Hamiltonian [2]

$$\hat{H}_{\rm R}' = \omega_{\rm c}\,\hat{a}^\dagger\hat{a} + \omega_{\rm q}\hat{\sigma}^+\hat{\sigma}^- + \Omega_{\rm R}(\hat{a}^\dagger + \hat{a})(\cos\theta\,\hat{\sigma}_x + \sin\theta\,\hat{\sigma}_z). \tag{18}$$

In this system both the number of excitations and parity symmetry are no longer conserved and transitions which are forbidden in natural atoms become available [64]. The angle θ as well as the qubit resonance frequency depend on the flux offset $\delta\Phi_{\rm q} \equiv \Phi_{\rm ext} - \Phi_0$, where $\Phi_{\rm ext}$ is the external magnetic flux threading the qubit and Φ_0 is the flux quantum. A flux offset $\delta\Phi_{\rm q} = 0$ implies $\theta = 0$. In this case $H_{\rm R}'$ reduces to the standard Rabi Hamiltonian (1). We choose the labeling of the eigenstates $|\tilde{i}\rangle$ and eigenvalues $\omega_{\tilde{j}}$ of $H_{\rm R}'$ such that $\omega_{\tilde{k}} > \omega_{\tilde{j}}$ for $\tilde{k} > \tilde{j}$.

The lowest eigenenergy offsets with respect to the ground energy $\omega_{\tilde{j}} - \omega_{\tilde{0}}$ as a function of the qubit transition frequency $\omega_{\rm q}$ are shown in figure 2. Looking at the numerically calculated eigenvectors, the first excited state, $|\tilde{1}\rangle$, contains a dominant contribution from the bare state $|g, 1\rangle$, ($|\tilde{1}\rangle \simeq |g, 1\rangle$). The figure also shows an avoided crossing when $\omega_{\rm q} \approx 2\omega_{\rm c}$. The splitting can be attributed to the resonant coupling of the states

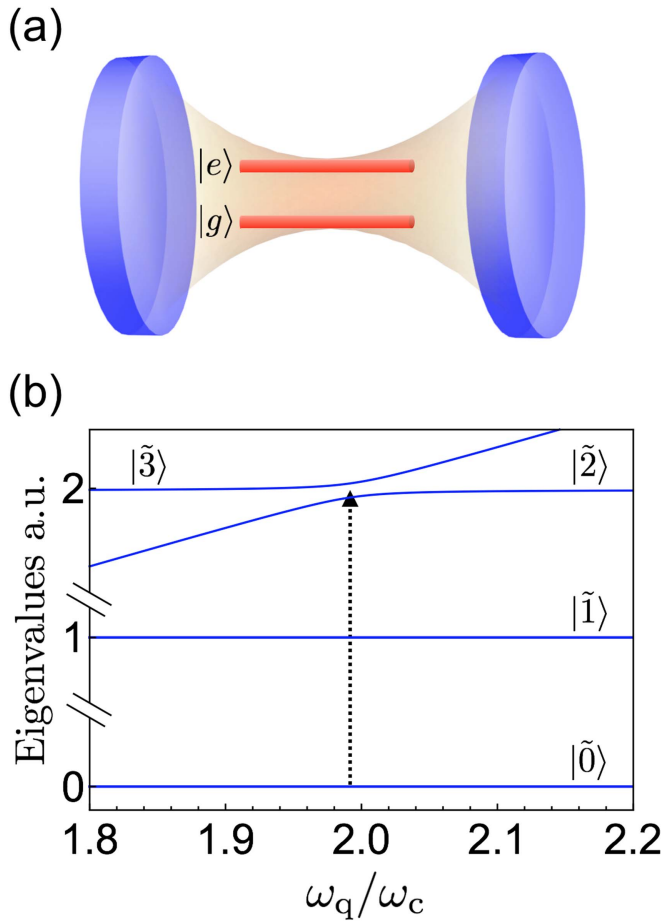

Figure 2. (a) Sketch of a cavity-embedded two-level system. (b) Frequency differences with respect to the ground state: $\omega_{\tilde{k}\tilde{0}} = \omega_{\tilde{k}} - \omega_{\tilde{0}}$ for the lowest-energy dressed states of $\hat{H}_R'$ as a function of the qubit transition frequency ω_q/ω_c. We consider a normalized coupling rate $\Omega_R/\omega_c = 0.15$ between the qubit and the resonator. In correspondence of the avoided level crossing (at $\omega_q \approx 2\omega_c$) a Gaussian pulse is sent with central frequency in the middle of the two split transition energies (black arrow).

$|e,\ 0\rangle$ and $|g,\ 2\rangle$, although the USC regime implies that the resulting dressed states $|\tilde{2}\rangle$ and $|\tilde{3}\rangle$ contain also small contributions from other bare states, as $|g,\ 1\rangle$ and $|e,\ 1\rangle$. This splitting cannot be found in the rotating wave approximation, where the coherent coupling between states with a different number of excitations is not allowed, nor does it occur with the standard Rabi Hamiltonian ($\theta = 0$).

We consider a system initially in the ground state. Excitation occurs by direct optical driving of the qubit via a microwave antenna. The corresponding driving Hamiltonian is

$$\hat{H}_d = \mathcal{E}(t)\cos(\omega t)\hat{\sigma}_x, \tag{19}$$

where $\mathcal{E}(t) = A\exp[-(t - t_0)^2/(2\tau^2)]/(\tau\sqrt{2\pi})$ describes a Gaussian pulse. Here A and τ are the amplitude and the standard deviation of the Gaussian pulse, respectively. We consider the zero-detuning case, corresponding to the minimum energy splitting $2\Omega_{\rm eff}$ between the two split levels ($|\tilde{2}\rangle$ and $|\tilde{3}\rangle$) in figure 2(b). The central frequency of the pulse has been chosen to be in the middle of the two split transition energies: $\omega = (\omega_{\tilde{3}} + \omega_{\tilde{2}})/2 - \omega_{\tilde{0}}$. If τ is much smaller than the effective Rabi period, $\tau \ll T_R = 2\pi/\Omega_{\rm eff}$, the driving pulse is able to generate an initial superposition with equal weights of the states $|\tilde{2}\rangle$ and $|\tilde{3}\rangle$, which will evolve displaying two-photon quantum vacuum oscillations [60]. Figure 3(a) displays the resulting qubit population (red dashed curve) and mean photon number (blue continuous) after a pulsed excitation with an effective pulse area $\mathcal{A} = \pi/3$. Figure 3(b) shows the normally-ordered variance of the two orthogonal output field quadratures $S_1^{(n)}$ (blue continuous curve) and $S_2^{(n)}$ (dotted red). Both the two quadratures display a significant amount of squeezing when the mean photon number is maximum. It is interesting to see that the periodicity of the two variances is twice the Rabi period T_R. This can be understood noticing that after the excitation, the quantum state is a superposition of the ground state $|\tilde{0}\rangle$ and the excited states $|\tilde{2}\rangle$ and $|\tilde{3}\rangle$. After one Rabi oscillation, the excited states acquire a π phase shift. A second Rabi oscillation is needed to recover the initial phase. The dynamics of the corresponding variances (not shown here) calculated by using $\hat{a}$ and $\hat{a}^\dagger$, instead of $\hat{x}^+$ and $\hat{x}^-$, are affected by fast oscillations.

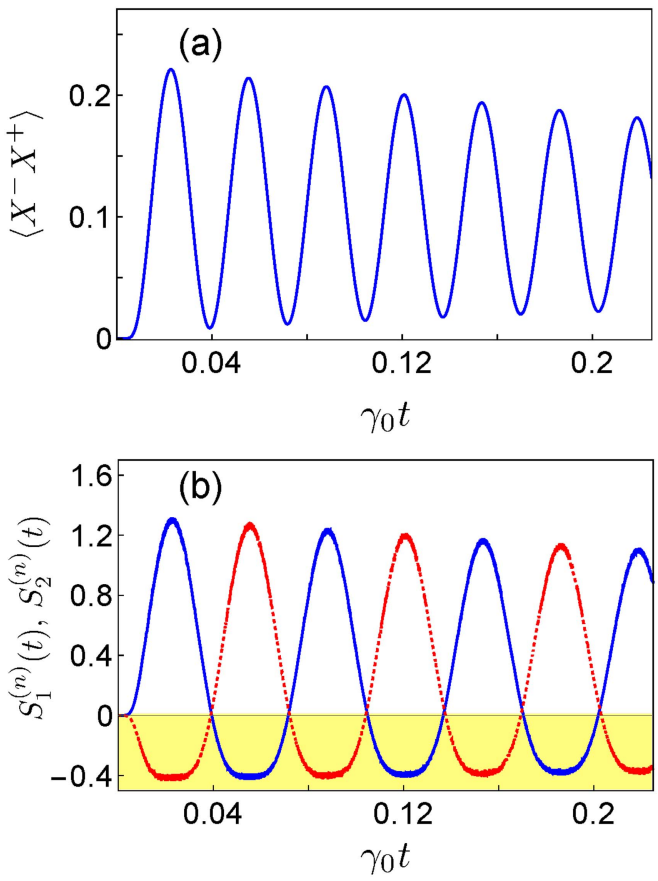

Figure 3. (a) Temporal evolution of the cavity mean photon number $\langle \hat{X}^- \hat{X}^+ \rangle$ (blue continuos curve) after the arrival of a Gaussian pulse exciting the qubit. The pulse has an affective area $\pi/3$ and central frequency $(\omega_{\tilde{3}} + \omega_{\tilde{2}})/2$. (b) Time evolution of the normally-ordered variances $S_1^{(n)}(t)$ (blue continuos curve) and $S_2^{(n)}(t)$ (red dashed curve). Here, the resonator and qubit damping rates are $\gamma_c = \gamma_q = 1.8 \times 10^{-4}\omega_c$. The yellow background, (shaded region) shows the region with negative ordinates corresponding to squeezed states.

This periodic and alternating squeezing of the two quadratures can be better understood by a simplified effective model assuming that

$$|\tilde{2}\rangle \simeq \frac{1}{\sqrt{2}}(|e,\,0\rangle + |g,\,2\rangle),$$
$$|\tilde{3}\rangle \simeq \frac{1}{\sqrt{2}}(|e,\,0\rangle - |g,\,2\rangle). \tag{20}$$

Considering the qubit initially prepared in the superposition state $|\psi(t=0)\rangle = \alpha|g,\,0\rangle + \beta|e,\,0\rangle$ (with $|\alpha|^2 + |\beta|^2 = 1$), the resulting time evolution of the system state is, to a good approximation,

$$|\psi(t)\rangle = \alpha|g,\,0\rangle + \beta[\cos(\Omega_{\rm eff}t)|e,\,0\rangle + \sin(\Omega_{\rm eff}t)|g,\,2\rangle], \tag{21}$$

where $2\Omega_{\rm eff}$ is the minimum energy splitting in figure 2(b). At $t = \pi/(2\Omega_{\rm eff})$, the resulting state is $|g\rangle(\alpha|0\rangle + \beta|2\rangle)$, which is a squeezed photon state, reaching a maximum squeezing for $\alpha \simeq 1/3$.

4.2. Cascade three-level system

We consider a three-level ($|s\rangle$, $|g\rangle$ and $|e\rangle$) atom-like system with the upper transition ($|g\rangle \leftrightarrow |e\rangle$) ultrastrongly coupled with a mode of the resonator and a lower transition which does not interact with the resonator, as schematically shown in figure 4. The peculiar optical properties of this system have been analyzed calculating the dynamics of the populations and of normal-order correlation functions [15, 65, 66]. The system Hamiltonian is

$$\hat{H} = \omega_c \hat{a}^\dagger \hat{a} + \sum_{\alpha=s,g,e} \omega_\alpha \hat{\sigma}_{\alpha\alpha} + \Omega_{\rm R}(\hat{a} + \hat{a}^\dagger)(\hat{\sigma}_{eg} + \hat{\sigma}_{ge}), \tag{22}$$

where ω_α ($\alpha = s,\,g,\,e$) are the bare frequencies of the atom-like relevant states, and $\sigma_{\alpha\beta} = |\alpha\rangle\langle\beta|$ describes the transition operators (projection operators if $\alpha = \beta$) involving the levels of the quantum emitter. The Hamiltonian can be separated as $\hat{H} = \hat{H}_{\rm R} + \hat{H}_s$, where $\hat{H}_{\rm R}$ is the well known Rabi Hamiltonian, equation (1), and $\hat{H}_s = \omega_s \hat{\sigma}_{ss}$. As a consequence, the total Hamiltonian is block-diagonal and its eigenstates can be separated

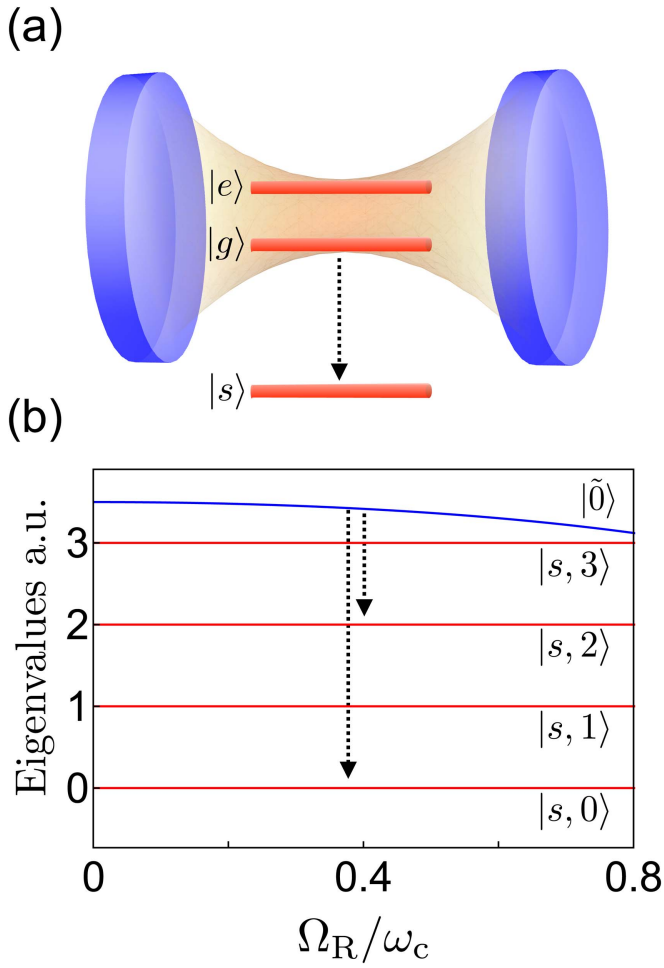

Figure 4. (a) Sketch of a cavity-embedded three-level system. Only the upper transition $|g\rangle \leftrightarrow |e\rangle$ interacts with the cavity mode. The lowest energy state of the three-level system is $|s\rangle$. (b) Energy spectrum of $\hat{H}$ as a function of the coupling strength Ω_R/ω_c, with $\omega_{gs} = 3.5\omega_c$ and $\omega_{eg} = \omega_c$. The red horizontal lines represent the non-interacting states $|s,\ n\rangle$, the blue curve is the lowest-energy atom-cavity dressed state $|\tilde{0}\rangle$. The black arrows indicate the transitions stimulated by the driving pulses.

into a non-interacting sector $|s,\ n\rangle$, with energy $\omega_s + n\omega_c$, where n labels the cavity photon number, and into dressed atom-cavity states $|\tilde{j}\rangle$, resulting from the diagonalization of the Rabi Hamiltonian. We consider the system initially prepared in the $|\tilde{0}\rangle$ state. Preparation can be accomplished by simply exciting the system initially in the ground state $|s,\ 0\rangle$ with a π pulse of central frequency $\omega_{\tilde{0}} - \omega_s$. Then the qubit is excited by two additional pulses with central frequencies $\omega_1 = \omega_{\tilde{0}} - 2\omega_c$ and $\omega_2 = \omega_{\tilde{0}} - \omega_s$. The driving Hamiltonian is

$$\hat{H}_d = [\mathcal{E}_1(t)\cos(\omega_1 t) + \mathcal{E}_2(t)\cos(\omega_2 t)](\hat{\sigma}_{gs} + \hat{\sigma}_{sg}), \tag{23}$$

where $\mathcal{E}_{1,2}(t) = A_{1,2}\exp[-(t - t_0)^2/(2\tau^2)]/(\tau\sqrt{2\pi})$ describes Gaussian pulses. While the transition $|\tilde{0}\rangle \rightarrow |s,\ 0\rangle$ is allowed in the weak-coupling regime or even in the absence of a resonator, the matrix element for the transition $|\tilde{0}\rangle \rightarrow |s,\ 2\rangle$ vanishes for a zero coupling rate and is negligible until Ω_R reaches at least 10% of ω_c. Specifically:

$$\begin{aligned}\langle s,\ 0|(\hat{\sigma}_{gs} + \hat{\sigma}_{sg})|\tilde{0}\rangle &= c_{g,0}^{\tilde{0}},\\ \langle s,\ 2|(\hat{\sigma}_{gs} + \hat{\sigma}_{sg})|\tilde{0}\rangle &= c_{g,2}^{\tilde{0}}.\end{aligned} \tag{24}$$

In order to obtain a quantum superposition $\cos\phi\ \ |s,\ 0\rangle + \sin\phi\ \ |s,\ 2\rangle$ via the dressed vacuum state $|\tilde{0}\rangle$, the pulse amplitudes have to satisfy the following relationship: $A_1 c_{g,0}^{\tilde{0}}/A_2 c_{g,2}^{\tilde{0}} = \tan\phi$. In order to obtain large squeezing, we choose the driving amplitude such that $\tan\phi \approx \sqrt{2}/2$, corresponding to the angle where squeezing for this superposition state is maximal.

Figure 5 shows the time evolution of the normally-ordered variances $S_1^{(n)}$ (blue upper curve) and $S_2^{(n)}$ (red lower curve) calculated using the correct positive and negative operators X^+ and X^-, with reference frequency $\Omega = \omega_c$. The squeezing displayed in figure 5 starts with the exact value for $t = 0$, $S_1^{(n)} = S_2^{(n)} = 0$, and it does not present any fictitious fast oscillation. On the contrary, with the use of the standard operators, see appendix C, the squeezing starts with a fictitious value less than zero and shows large fictitious oscillations.

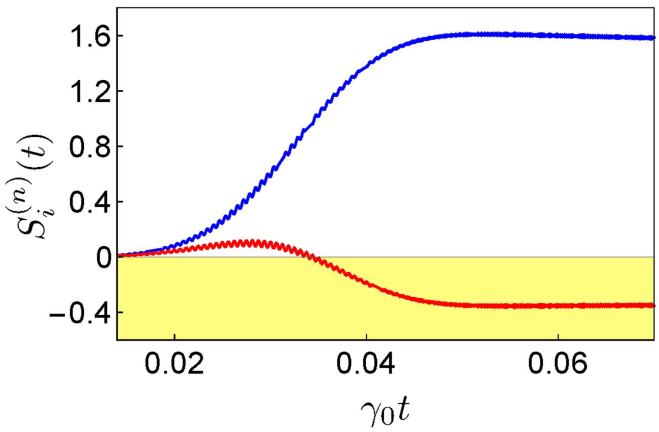

Figure 5. Time evolution of the normally-ordered variances $S_1^{(n)}$ (blue upper curve) and $S_2^{(n)}$ (red lower curve) calculated using the correct positive and negative operators for reference frequency $\Omega = \omega_c$. The system is initially prepared in the lowest-energy dressed state $|\tilde{0}\rangle$. The qubit is excited by two pulses with central frequencies $\omega_1 = \omega_{\tilde{0}} - 2\omega_c$ and $\omega_2 = \omega_{\tilde{0}} - \omega_s$, at the time $\gamma_0 t_1 = 2.6 \times 10^{-2}$ and $\gamma_0 t_2 = 3.8 \times 10^{-2}$, respectively, and with amplitude such that $\tan\phi \approx \sqrt{2}/2$. The damping rates are $\gamma_c = \gamma_{eg} = \gamma_{gs} = 2 \times 10^{-4}\omega_c$, and the coupling constant is $\Omega_R = 0.4\omega_c$. Other parameters are the same as in figure 4(b).

5. Conclusions

We have derived a generalized theory of the output field-quadrature measurements and squeezing in cavity-QED systems, valid for arbitrary cavity-atom coupling rates. In the USC regime, where the counter-rotating terms cannot be ignored, the standard theory predicts a large amount of squeezing in the output field, even when the system is in its ground state. Here we have shown that, in this case, no squeezing can be detected in the output field-quadratures, independently of the system details. We have applied our theoretical approach to study the output squeezing produced by an artificial two-level atom embedded in a coherently excited cavity. We showed that, a large degree of squeezing can be obtained with this elementary quantum system. We also studied the output field-quadratures from a cavity interacting in the USC regime with the upper transition of a cascade-type three-level system. The numerical results have been compared with the standard calculations of output squeezing (see figure 5). The approach proposed here can be directly applied also to resonators displaying ultrastrong optical nonlinearities [67]. This work extends the possibilty of predicting and analyzing output-field correlations when optical resonators interact very strongly with other quantum systems.

Acknowledgments

We thank Professor Adam Miranowicz for very useful discussions. This work is partially supported by the RIKEN iTHES Project, the MURI Center for Dynamic Magneto-Optics via the AFOSR award number FA9550-14-1-0040, the IMPACT program of JST, a Grant-in-Aid for Scientific Research (A), CREST, the John Templeton Foundation, and from the MPNS COST Action MP1403 Nanoscale Quantum Optics.

Appendix A. Commutation relations

Here we derive the commutation relation (12) among the positive component of the input field $\hat{A}_{\rm in}^{+}(t)$ and any system operator $\hat{Y}(t)$. The calculation for the negative component can then be obtained simply by Hermitian conjugation. The total Hamiltonian that describes the coupling between the system and a bath of harmonic oscillators is

$$\hat{H} = \hat{H}_{\rm S} + \hat{H}_{\rm F} + \hat{H}_{\rm SF}, \tag{A1}$$

where $\hat{H}_{\rm S}$ is an arbitrary system Hamiltonian, $\hat{H}_{\rm F}$ is the Hamiltonian that describes the bath:

$$\hat{H}_{\rm F} = \sum_n \hbar\omega_n \left(\hat{b}_n^{\dagger}\hat{b}_n + \frac{1}{2}\right), \tag{A2}$$

and the interaction Hamiltonian $\hat{H}_{\rm SF}$ is

$$\hat{H}_{\rm SF} = {\rm i}\sum_n k_n \sqrt{\frac{\hbar\omega_n}{2}}\,(\hat{b}_n - \hat{b}_n)\hat{X}, \tag{A3}$$

where $\hat{X}$ is the system variable that interacts with the bath. In the basis that diagonalizes the system Hamiltonian $\hat{H}_{\rm S}$, we have $\hat{X} = \hat{X}^+ + \hat{X}^-$, with $\hat{X}^+ = \sum_{i<j} X_{ij}|i\rangle\langle j|$ and $\hat{X}^- = (\hat{X}^+)^\dagger$. In the continuum limit for n and in the RWA, the interaction Hamiltonian in equation (A3), can be expressed as

$$\hat{H}_{\rm SF} = {\rm i}\int_0^\infty {\rm d}\omega\, k(\omega)\sqrt{\frac{\hbar\omega}{2}}\,[\hat{X}^-\hat{b}(\omega) - \hat{X}^+\hat{b}^\dagger(\omega)]. \tag{A4}$$

We observe that the RWA has been applied only after expressing the system operators in equation (A3) in the dressed basis, so that the resulting operators $\hat{X}^\pm$ have a definite positive/negative frequency. Observing that the input field $\hat{A}^+_{\rm in}(t)$ is a continuous superposition of the initial-time destruction operators $\hat{b}(\omega, t_0)$ (see equation (6)), we can obtain an expression for it by solving the following Heisenberg equation of motion:

$$\dot{\hat{b}}(\omega) = \frac{\rm i}{\hbar}[\hat{H}, \hat{b}(\omega)]. \tag{A5}$$

We obtain:

$$\hat{b}(\omega, t_0) = \hat{b}(\omega, t){\rm e}^{{\rm i}\omega(t-t_0)} + k(\omega)\sqrt{\frac{\omega}{2\hbar}}\int_{t_0}^t {\rm d}t'{\rm e}^{-{\rm i}\omega(t_0-t')}\hat{X}^+(t'). \tag{A6}$$

Now we can calculate $[\hat{Y}(t), \hat{A}^+_{\rm in}(t'')]$. From the definition of the positive-frequency component of the input field $\hat{A}^+_{\rm in}(t)$, we obtain:

$$[\hat{Y}(t), \hat{A}^+_{\rm in}(t'')] = \frac{1}{2}\int_0^\infty {\rm d}\omega\sqrt{\frac{\hbar}{\pi\omega\nu}}\,{\rm e}^{-{\rm i}\omega(t''-t_0)}[\hat{Y}(t), \hat{b}(\omega, t_0)]. \tag{A7}$$

Replacing $\hat{b}(\omega, t_0)$ from equation (A6):

$$[\hat{Y}(t), \hat{A}^+_{\rm in}(t'')] = \frac{1}{2\sqrt{2\pi\nu}}\int_0^\infty {\rm d}\omega\, k(\omega)\int_{t_0}^t {\rm d}t'{\rm e}^{-{\rm i}\omega(t''-t')}[\hat{Y}(t), \hat{X}^+(t')]. \tag{A8}$$

Applying the first Markov approximation $k(\omega) = \sqrt{2\gamma/\pi}$, the above expression becomes

$$[\hat{Y}(t), \hat{A}^+_{\rm in}(t'')] = \frac{1}{2\pi}\sqrt{\frac{\gamma}{\nu}}\int_{t_0}^t {\rm d}t'[\hat{Y}(t), \hat{X}^+(t')]\int_0^\infty {\rm d}\omega\, {\rm e}^{-{\rm i}\omega(t''-t')}. \tag{A9}$$

We notice that the positive-frequency operator $X^+(t')$ on the r.h.s. of equation (A9) is a superposition of oscillating phases ${\rm e}^{-{\rm i}\omega' t'}$ (being ω' a generic positive frequency). Hence the time integral on the r.h.s. of equation (A9) contains terms oscillating as ${\rm e}^{{\rm i}(\omega-\omega')t'}$. Those slowly-oscillating terms with $\omega \approx \omega'$ provide the larger contributions to the integral. If we extend the frequency integral to the $-\infty$ limit, we are adding rapidly-oscillating terms ${\rm e}^{-{\rm i}(|\omega|+\omega')t'}$, which provide negligible contributions. After the integral is extended to the $-\infty$ limit, we observe that the ω-integral is now equal to $2\pi\delta(t - t')$, and we finally obtain:

$$[\hat{Y}(t), \hat{A}^+_{\rm in}(s)] = \sqrt{\frac{\gamma}{\nu}}\,u(t-s)[\hat{Y}(t), \hat{X}^+(t)], \tag{A10}$$

where $u(t - s)$ is equal to 1 if $t > s$, $\frac{1}{2}$ if $t = s$, and 0 if $t < s$.

Appendix B. Master equation

In the USC regime, owing to the high ratio $\Omega_{\rm R}/\omega_{\rm c}$, the standard approach fails to correctly describe the dissipation processes and leads to unphysical results as well. In particular, it predicts that even at $T = 0$, relaxation would drive the system out of its ground state $|G\rangle$ generating photons in excess to those already present.

The right procedure that solves such issues consists in taking into account the atom-cavity coupling when deriving the master equation after expressing the Hamiltonian of the system in a basis formed by the eigenstates $|j\rangle$ of the Rabi Hamiltonian $\hat{H}_{\rm R}$. The dissipation baths are still treated in the Born-Markov approximation. Following this procedure it is possible to obtain the master equation in the dressed picture [62]. For a $T = 0$ reservoir, one obtains:

$$\dot{\hat{\rho}}(t) = -{\rm i}[\hat{H}_{\rm S}, \hat{\rho}(t)] + \mathcal{L}_{\rm a}\hat{\rho}(t) + \mathcal{L}_x\hat{\rho}(t). \tag{B1}$$

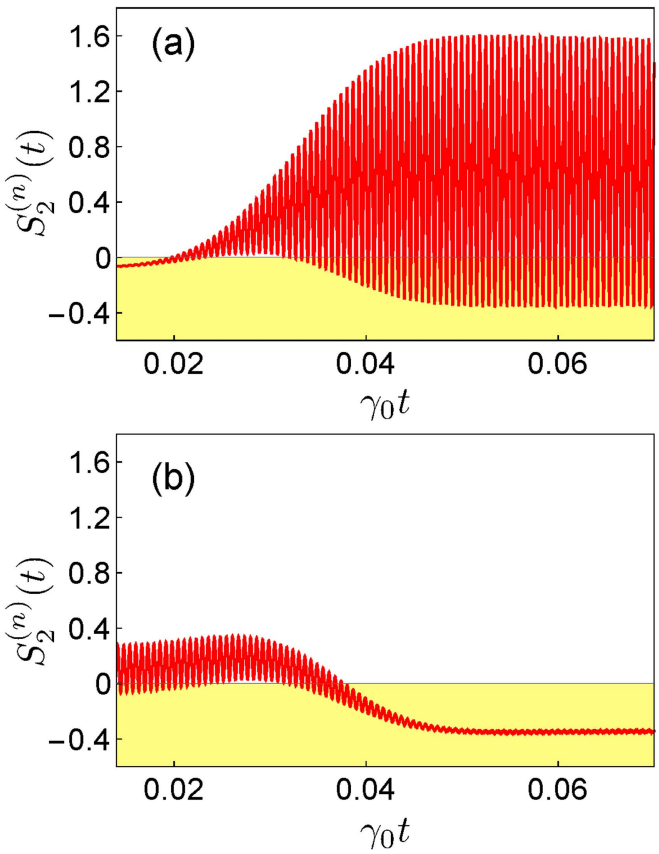

Figure C1. Time evolution of the normally-ordered variances $S_2^{(n)}$ in the case discussed in section 4.2, calculated with the standard operators ($\hat{x}^+ = \hat{a}$). The parameters are the same used in figure 5 in section 4.2. The variances $S_2^{(n)}$ are calculated with reference frequency (a) $\Omega = 0$ and (b) $\Omega = \omega_c$.

Here $\mathcal{L}_a$ and $\mathcal{L}_x$ are the Liouvillian superoperators correctly describing the losses of the system where $\mathcal{L}_s\hat{\rho}(t) = \sum_{j,k>j}\Gamma_s^{jk}\mathcal{D}[|j\rangle\langle k|]\hat{\rho}(t)$ for $s = a,\ \sigma_-$ and $\mathcal{D}[\hat{O}]\hat{\rho} = \frac{1}{2}(2\hat{O}\hat{\rho}\hat{O}^\dagger - \hat{\rho}\hat{O}^\dagger\hat{O} - \hat{O}^\dagger\hat{O}\hat{\rho})$. In the limit $\Omega_R \to 0$, standard dissipators are recovered.

The relaxation rates $\Gamma_s^{jk} = 2\pi d_s(\Delta_{kj})\alpha_s^2(\Delta_{kj})|C_{jk}^s|^2$ depend on the density of states of the baths $d_s(\Delta_{kj})$ and the system-bath coupling strength $\alpha_s(\Delta_{kj})$ at the respective transition frequency $\Delta_{kj} \equiv \omega_k - \omega_j$ as well as on the transition coefficients $C_{jk} = \langle j|\hat{s} + \hat{s}^\dagger|k\rangle$ ($\hat{s} = \hat{a},\ \hat{\sigma}_-$). These relaxation coefficients can be interpreted as the full width at half maximum of each $|k\rangle \to |j\rangle$ transition. In the Born-Markov approximation the density of states of the baths can be considered a slowly varying function of the transition frequencies, so that we can safely assume it to be constant as well as the coupling strength.

Appendix C. Standard numerically-calculated squeezing

In section 4.2 we have numerically calculated the squeezing for the output field generated by the dynamics of a three-level system when the two upper levels are ultrastrongly coupled with a cavity mode. We obtain a quantum superposition between the $|s,\ 0\rangle$ and $|s,\ 2\rangle$ states via the dressed vacuum state $|\tilde{0}\rangle$ sending two pulses with central frequencies $\omega_1 = \omega_{\tilde{0}} - 2\omega_c$ and $\omega_2 = \omega_{\tilde{0}} - \omega_s$.

Figures C1(a) and (b) display the time evolution of the variances $S_2^{(n)}$ calculated by using the standard quadrature-field operators in terms of the destruction and creation operators $\hat{a}$ and $\hat{a}^\dagger$ for the cavity field.

This result can be compared with figure 5 displaying the time evolution of the variances $S_1^{(n)}$ (blue curve) and $S_2^{(n)}$ (red curve) obtained using the correct positive and negative field operators. The behavior of $S_2^{(n)}(t)$ in figure C1(a) starts with a fictitious value less than zero, while in figure 5 correctly starts from 0. The variance $S_2^{(n)}$ in figure C1(a) has been calculated by using the reference frequency $\Omega = 0$. Figure C1(b) has been obtained by using $\Omega = \omega_c$. Figures C1(a) and (b) show that it is not possible to eliminate fast and large-amplitude fictitious oscillations, as well as the fictious initial squeezing within the standard approach.

References

[1] Forn-Díaz P, Lisenfeld J, Marcos D, García-Ripoll J J, Solano E, Harmans C J P M and Mooij J E 2010 Observation of the Bloch-Siegert shift in a qubit-oscillator system in the ultrastrong coupling regime *Phys. Rev. Lett.* **105** 237001
[2] Niemczyk T *et al* 2010 Circuit quantum electrodynamics in the ultrastrong-coupling regime *Nat. Phys.* **6** 772–6
[3] Todorov Y, Andrews A M, Colombelli R, De Liberato S, Ciuti C, Klang P, Strasser G and Sirtori C 2010 Ultrastrong light-matter coupling regime with polariton dots *Phys. Rev. Lett.* **105** 196402
[4] Schwartz T, Hutchison J A, Genet C and Ebbesen T W 2011 Reversible switching of ultrastrong light-molecule coupling *Phys. Rev. Lett.* **106** 196405
[5] Scalari G *et al* 2012 Ultrastrong coupling of the cyclotron transition of a 2D electron gas to a THz metamaterial *Science* **335** 1323–6
[6] Geiser M, Castellano F, Scalari G, Beck M, Nevou L and Faist J 2012 Ultrastrong coupling regime and plasmon polaritons in parabolic semiconductor quantum wells *Phys. Rev. Lett.* **108** 106402
[7] Kéna-Cohen S, Maier S A and Bradley D D C 2013 Ultrastrongly coupled exciton-polaritons in metal-clad organic semiconductor microcavities *Adv. Opt. Mater.* **1** 827–33
[8] Gambino S *et al* 2014 Exploring light–matter interaction phenomena under ultrastrong coupling regime *ACS Photon.* **1** 1042–8
[9] Dimer F, Estienne B, Parkins A S and Carmichael H J 2007 Proposed realization of the dicke-model quantum phase transition in an optical cavity qed system *Phys. Rev.* A **75** 013804
[10] De Liberato S, Ciuti C and Carusotto I 2007 Quantum vacuum radiation spectra from a semiconductor microcavity with a time-modulated vacuum Rabi frequency *Phys. Rev. Lett.* **98** 103602
[11] Cao X, You J Q, Zheng H, Kofman A G and Nori F 2010 Dynamics and quantum Zeno effect for a qubit in either a low-or high-frequency bath beyond the rotating-wave approximation *Phys. Rev.* A **82** 022119
[12] Cao X, You J Q, Zheng H and Nori F 2011 A qubit strongly coupled to a resonant cavity: asymmetry of the spontaneous emission spectrum beyond the rotating wave approximation *New J. Phys.* **13** 073002
[13] Ridolfo A, Leib M, Savasta S and Hartmann M J 2012 Photon blockade in the ultrastrong coupling regime *Phys. Rev. Lett.* **109** 193602
[14] Ridolfo A, Savasta S and Hartmann M J 2013 Nonclassical radiation from thermal cavities in the ultrastrong coupling regime *Phys. Rev. Lett.* **110** 163601
[15] Stassi R, Ridolfo A, Di Stefano O, Hartmann M J and Savasta S 2013 Spontaneous conversion from virtual to real photons in the ultrastrong-coupling regime *Phys. Rev. Lett.* **110** 243601
[16] Sánchez-Burillo E, Zueco D, Garcia-Ripoll J J and Martín-Moreno L 2014 Scattering in the ultrastrong regime: nonlinear optics with one photon *Phys. Rev. Lett.* **113** 263604
[17] Garziano L, Stassi R, Ridolfo A, Di Stefano O and Savasta S 2014 Vacuum-induced symmetry breaking in a superconducting quantum circuit *Phys. Rev.* A **90** 043817
[18] Cacciola A, Di Stefano O, Stassi R, Saija R and Savasta S 2014 Ultrastrong coupling of plasmons and excitons in a nanoshell *ACS Nano* **8** 11483–92
[19] Ciuti C and Carusotto I 2006 Input-output theory of cavities in the ultrastrong coupling regime: the case of time-independent cavity parameters *Phys. Rev.* A **74** 033811
[20] Bamba M and Ogawa T 2014 Recipe for the hamiltonian of system-environment coupling applicable to the ultrastrong-light-matter-interaction regime *Phys. Rev.* A **89** 023817
[21] Ashhab S and Nori F 2010 Qubit-oscillator systems in the ultrastrong-coupling regime and their potential for preparing nonclassical states *Phys. Rev.* A **81** 042311
[22] Garziano L, Ridolfo A, Stassi R, Di Stefano O and Savasta S 2013 Switching on and off of ultrastrong light–matter interaction: photon statistics of quantum vacuum radiation *Phys. Rev.* A **88** 063829
[23] Lvovsky A I and Raymer M G 2009 Continuous-variable optical quantum-state tomography *Rev. Mod. Phys.* **81** 299
[24] Wiseman H M and Milburn G J 1993 Quantum theory of field-quadrature measurements *Phys. Rev.* A **47** 642
[25] Mallet F, Castellanos-Beltran M A, Ku H S, Glancy S, Knill E, Irwin K D, Hilton G C, Vale L R and Lehnert K W 2011 Quantum state tomography of an itinerant squeezed microwave field *Phys. Rev. Lett.* **106** 220502
[26] Drummond P D and Ficek Z 2004 *Quantum Squeezing* vol 27 (Berlin: Springer)
[27] Walls D F and Milburn G J 1994 *Quantum Optics* (Berlin: Springer)
[28] Mandel L and Wolf E 1995 *Optical Coherence and Quantum Optics* (Cambridge: Cambridge University Press)
[29] Scully M O and Zubairy M S 1997 *Quantum Optics* (Cambridge: Cambridge University Press)
[30] Bartkowiak M, Wu L-A and Miranowicz A 2014 Quantum circuits for amplification of Kerr nonlinearity via quadrature squeezing *J. Phys. B: At. Mol. Opt. Phys.* **47** 145501
[31] Ma J, Wang X, Sun C P and Nori F 2011 Quantum spin squeezing *Phys. Rep.* **509** 89–165
[32] Zagoskin A M, Ilichev E, McCutcheon M W, Young J F and Nori F 2008 Controlled generation of squeezed states of microwave radiation in a superconducting resonant circuit *Phys. Rev. Lett.* **101** 253602
[33] Johansson J R, Johansson G, Wilson C M and Nori F 2010 Dynamical Casimir effect in superconducting microwave circuits *Phys. Rev.* A **82** 052509
[34] Wilson C M, Johansson G, Pourkabirian A, Simoen M, Johansson J R, Duty T, Nori F and Delsing P 2011 Observation of the dynamical Casimir effect in a superconducting circuit *Nature* **479** 376–9
[35] Nation P D, Johansson J R, Blencowe M P and Nori F 2012 Stimulating uncertainty: amplifying the quantum vacuum with superconducting circuits *Rev. Mod. Phys.* **84** 1–24
[36] Slavík R *et al* 2010 All-optical phase and amplitude regenerator for next-generation telecommunications systems *Nat. Photon.* **4** 690–5
[37] Caves C M 1981 Quantum-mechanical noise in an interferometer *Phys. Rev.* D **23** 1693
[38] Braunstein S L and Loock P Van 2005 Quantum information with continuous variables *Rev. Mod. Phys.* **77** 513
[39] Castellanos-Beltran M A, Irwin K D, Hilton G C, Vale L R and Lehnert K W 2008 Amplification and squeezing of quantum noise with a tunable Josephson metamaterial *Nat. Phys.* **4** 929–31
[40] Giovannetti V, Lloyd S and Maccone L 2011 Advances in quantum metrology *Nat. Photon.* **5** 222–9
[41] Vahlbruch H, Mehmet M, Chelkowski S, Hage B, Franzen A, Lastzka N, Gossler S, Danzmann K and Schnabel R 2008 Observation of squeezed light with 10 dB quantum-noise reduction *Phys. Rev. Lett.* **100** 033602
[42] Eichler C, Bozyigit D, Lang C, Baur M, Steffen L, Fink J M, Filipp S and Wallraff A 2011 Observation of two-mode squeezing in the microwave frequency domain *Phys. Rev. Lett.* **107** 113601
[43] Flurin E, Roch N, Mallet F, Devoret M H and Huard B 2012 Generating entangled microwave radiation over two transmission lines *Phys. Rev. Lett.* **109** 183901

[44] Walls D F and Zoller P 1981 Reduced quantum fluctuations in resonance fluorescence *Phys. Rev. Lett.* **47** 709
[45] Meystre P and Zubairy M S 1982 Squeezed states in the Jaynes–Cummings model *Phys. Lett.* A **89** 390–2
[46] Carmichael H J 1985 Photon antibunching and squeezing for a single atom in a resonant cavity *Phys. Rev. Lett.* **55** 2790–3
[47] Raizen M G, Orozco L A, Xiao M, Boyd T L and Kimble H J 1987 Squeezed-state generation by the normal modes of a coupled system *Phys. Rev. Lett.* **59** 198–201
[48] Nha H 2003 Squeezing effect in a driven coupled-oscillator system: a dual role of damping *Phys. Rev.* A **67** 023801
[49] Schulte C H H, Hansom J, Jones A E, Matthiesen C, Le Gall C and Atatüre M 2015 Quadrature squeezed photons from a two-level system *Nature* **525** 222–5
[50] Collett M J and Gardiner C W 1984 Squeezing of intracavity and traveling-wave light fields produced in parametric amplification *Phys. Rev.* A **30** 1386
[51] Gardiner C W and Collett M J 1985 Input and output in damped quantum systems: quantum stochastic differential equations and the master equation *Phys. Rev.* A **31** 3761
[52] Bozyigit D *et al* 2011 Antibunching of microwave-frequency photons observed in correlation measurements using linear detectors *Nat. Phys.* **7** 154–8
[53] Eichler C, Bozyigit D, Lang C, Steffen L, Fink J and Wallraff A 2011 Experimental state tomography of itinerant single microwave photons *Phys. Rev. Lett.* **106** 220503
[54] Mariantoni M, Menzel E P, Deppe F, Araque Caballero M Á, Baust A, Niemczyk T, Hoffmann E, Solano E, Marx A and Gross R 2010 Planck spectroscopy and quantum noise of microwave beam splitters *Phys. Rev. Lett.* **105** 133601
[55] Rabi I I 1936 On the process of space quantization *Phys. Rev.* **49** 324
[56] Rabi I I 1937 Space quantization in a gyrating magnetic field *Phys. Rev.* **51** 652
[57] Gardiner C and Zoller P 2004 *Quantum Noise* vol 56 (Berlin: Springer)
[58] Glauber R J and Lewenstein M 1991 Quantum optics of dielectric media *Phys. Rev.* A **43** 467
[59] Savasta S and Girlanda R 1996 Quantum description of the input and output electromagnetic fields in a polarizable confined system *Phys. Rev.* A **53** 2716
[60] Garziano L, Stassi R, Macrì V, Frisk Kockum A, Savasta S and Nori F 2015 Multiphoton quantum Rabi oscillations in ultrastrong cavity QED *Phys. Rev.* A **92** 063830
[61] Breuer H-P and Petruccione F 2002 *The Theory of Open Quantum Systems* (Oxford: Oxford University Press)
[62] Beaudoin F, Gambetta J M and Blais A 2011 Dissipation and ultrastrong coupling in circuit QED *Phys. Rev.* A **84** 043832
[63] Ma K K W and Law C K 2015 Three-photon resonance and adiabatic passage in the large-detuning Rabi model *Phys. Rev.* A **92** 023842
[64] Liu Y X, You J Q, Wei L F, Sun C P and Nori F 2005 Optical selection rules and phase-dependent adiabatic state control in a superconducting quantum circuit *Phys. Rev. Lett.* **95** 087001
[65] Ridolfo A, Vilardi R, Di Stefano O, Portolan S and Savasta S 2011 All optical switch of vacuum rabi oscillations: the ultrafast quantum eraser *Phys. Rev. Lett.* **106** 013601
[66] Huang J-F and Law C K 2014 Photon emission via vacuum-dressed intermediate states under ultrastrong coupling *Phys. Rev.* A **89** 033827
[67] Ridolfo A, del Valle E and Hartmann M J 2013 Photon correlations from ultrastrong optical nonlinearities *Phys. Rev.* A **88** 063812